

# Single-cell transcriptomics defines Dot1L interacting partners and downstream target genes in the mouse molar dental pulp

ROSA GUZZO<sup>1</sup>, BADAM ENKHMANDAKH<sup>2</sup>, TIMOTHY BECKER<sup>3</sup>, PUJAN JOSHI<sup>4</sup>, PAUL ROBSON<sup>5</sup>, ANUSHREE VIJAYKUMAR<sup>6</sup>, MINA MINA<sup>6</sup>, DONG-GUK SHIN<sup>4</sup>, DASHZEVEG BAYARSAIHAN<sup>\*2,7</sup>

<sup>1</sup>Department of Neuroscience, University of Connecticut Health Center, Farmington, CT, USA, <sup>2</sup>Center for Regenerative Medicine and Skeletal Development, Department of Reconstructive Sciences, University of Connecticut Health Center, Farmington, CT, USA, <sup>3</sup>Computing Sciences Department, University of Hartford, West Hartford, CT, USA, <sup>4</sup>Computer Science and Engineering Department, University of Connecticut, Storrs, CT, USA, <sup>5</sup>The Jackson Laboratory for Genomic Medicine, Farmington, CT, USA, <sup>6</sup>Department of Craniofacial Sciences, University of Connecticut Health Center, Farmington, CT, USA, <sup>7</sup>Institute for System Genomics, University of Connecticut, Storrs, CT, USA

**ABSTRACT** Although histone methyltransferases are implicated in many key developmental processes, the contribution of individual chromatin modifiers in dental tissues is not well understood. Using single-cell RNA sequencing, we examined the expression profiles of the disruptor of telomeric silencing 1-like (*Dot1L*) gene in the postnatal day 5 mouse molar dental pulp. *Dot1L* is the only known enzyme that methylates histone 3 on lysine 79, a modification associated with gene expression. Our research revealed 15 distinct clusters representing different populations of mesenchymal stromal cells (MSCs), immune cells, pericytes, ameloblasts and endothelial cells. We documented heterogeneity in gene expression across different subpopulations of MSCs, a good indicator that these stromal progenitors undergo different phases of osteogenic differentiation. Interestingly, although *Dot1L* was broadly expressed across all cell clusters within the molar dental pulp, our analyses indicated specific enrichment of *Dot1L* within two clusters of MSCs, as well as cell clusters characterized as ameloblasts and endothelial cells. Moreover, we detected *Dot1L* co-expression with protein interactors involved in epigenetic activation such as *Setd2*, *Sirt1*, *Brd4*, *Isw1*, *Bptf* and *Suv39h1*. In addition, *Dot1L* was co-expressed with *Eed2*, *Cbx3* and *Dnmt1*, which encode epigenetic factors associated with gene silencing and heterochromatin formation. *Dot1L* was co-expressed with downstream targets of the insulin growth factor and WNT signaling pathways, as well as genes involved in cell cycle progression. Collectively, our results suggest that *Dot1L* may play key roles in orchestrating lineage-specific gene expression during MSC differentiation.

**KEYWORDS:** *Dot1L*, histone methyltransferase, dental pulp, stem cells, H3K79me2

## Introduction

The dental pulp is the neurovascular bundle central to each tooth, and consists of nerve fibers, blood vessels and stromal cells (Sui *et al.*, 2019). The dental pulp is composed of a heterogenous population of MSCs exhibiting self-renewal, a high capacity for multi-lineage differentiation, and the potential to regenerate a dentin/pulp-like complex (Tsutsui, 2020). The fate of the dental pulp cells is regulated by multiple transcription factors (e.g., *Msx1*, *Lef1*, *Pitx2* and *Runx2*) and growth factors (e.g., basic fibroblast growth factor, transforming growth factor- $\beta$  and bone morphogenic proteins) (Zhang *et al.*, 2005). However, an important issue that

remains poorly addressed is uncovering the epigenetic regulatory mechanisms involved in the renewal and differentiation of dental pulp progenitors.

A highly conserved histone methyltransferase known as disruptor of telomeric silencing 1-like (*Dot1L*) plays a critical role in several cellular processes including cell cycle regulation, DNA damage repair, transcriptional elongation, cell differentiation and reprogramming (Sarno *et al.*, 2020; Steger *et al.*, 2008; Barry *et al.*, 2009; Kim *et al.*, 2014; Yang *et al.*, 2019; FitzGerald *et al.*, 2011; Wakeman *et al.*, 2012). *Dot1L* itself is enriched at actively transcribed genes through its interaction with phosphorylated C-terminal domain of RNA polymerase II (Steger *et al.*, 2008; Kim *et al.*, 2012), and serves

\*Address correspondence to: Dashzeveg Bayarsaihan. Center for Regenerative Medicine and Skeletal Development, Department of Reconstructive Sciences, University of Connecticut Health Center, 263 Farmington Avenue, Farmington, CT 06030, USA. E-mail: dashzeveg@uchc.edu

Submitted: 8 November, 2022; Accepted: 21 February, 2023; Published online: 21 February, 2023.

as the only enzyme that catalyzes the mono-, di- and tri methylation of histone 3 on lysine residue 79 (H3K79) (Feng et al., 2002). Enrichment of H3K79me2/3 within gene bodies is positively correlated with active transcription. Notably, a genome-wide analysis also revealed that H3K79me2 is deposited within gene regulatory sequences including enhancers and promoters (Wood et al., 2018; Ferrari et al., 2020). Mechanistically, Dot1L forms a complex with other factors such as AF10, AF17 and ENL to regulate transcription elongation in regions of active transcription. Recent studies suggest that Dot1L may also regulate transcriptional initiation by recruiting transcription factor IID (Wu et al., 2021). The interaction of Dot1L with mixed lineage leukemia (MLL) recruits RNA polymerase II to unmethylated CpG-rich promoters by forming a functional complex with the AF4/ENL/P-TEFb complex, MOZ and p300/CBP histone acetyl transferases (Miyamoto et al., 2020).

The essential role for Dot1L in mammalian development has been well-documented. Germline disruption of *Dot1L* and loss of H3K79me2 in mice results in mid-gestational lethality, which is attributed to defective extraembryonic vascular network formation, impaired hematopoietic development and cardiac hypertrophy (Duan et al., 2016; Feng et al., 2010). Multiple studies underscore the importance of meticulously regulated Dot1L function in establishing cell-type-specific transcriptional programs during differentiation. Several lines of evidence suggest that inhibition of Dot1L activity in progenitor populations biases the transcriptome from a stemness to a differentiation-mediating transcriptional program. For example, deficiency of Dot1L in the central nervous system reduces the number of neural progenitors, impairs neurogenesis and alters the distribution of neuronal subtypes (Franz et al., 2019; Bovio et al., 2019; Gray de Cristoforis et al., 2020). Yoo et al., determined that Dot1L function in blood endothelial cells or lymphatic progenitors ensures normal lymphatic development and function (Yoo et al., 2020). In the skeletal system, we previously demonstrated that early expression of *Dot1L* in limb mesenchymal progenitors provides regulatory control of endochondral bone growth and development through control of chondrocyte proliferation and differentiation

(Sutter et al., 2021). Our research further implicated Dot1L in the regulation of key signaling pathways and associated genes involved in proliferation, as well as cell cycle checkpoint control in growth plate chondrocytes.

The epigenetic control of dental progenitors by Dot1L remains unexplored. Thus, in the present study, we performed single-cell RNA sequencing (scRNA-seq) to gain new insights into the mechanistic contributions of Dot1L in early postnatal mouse molar dental pulp. Our analysis generated transcriptomic signatures demarcating 15 distinct cell clusters within the molar dental pulp, including ameloblasts, vascular endothelial blood cells, pericytes and immune cells, as well as multiple subpopulations of MSCs at various stages of osteogenic differentiation. Notably, our analysis of the transcriptionally distinct cell populations that make up the mouse molar pulp revealed enrichment of *Dot1L* within cell clusters representing MSCs. We showed that *Dot1L* co-expresses with genes encoding the epigenetic factors *Setd2*, *Sirt1*, *Suv39h1*, *Iws1*, *Pbrm1* and *Bptf*, which are associated with transcriptional activation. Interestingly, *Dot1L* co-expresses with genes encoding repressive epigenetic factors involved in DNA methylation and heterochromatin organization such as *Dnmt1*, *Eed*, *Suv39h1* and *Cbx3*. We also noted that *Dot1L* co-expresses with downstream target genes associated with insulin growth factor (IGF) and WNT signaling and cell cycle progression. Taken together, our research provides novel insights into the role of Dot1L in the lineage commitment of MSCs in the mouse molar dental pulp.

## Results

### Single-cell RNA analysis of MSCs in the mouse molar dental pulp

We identified 15 distinct cell clusters in the dental pulp of mouse molars based on the differential expression of marker genes (summarized in Fig. 1A). Based on the expression of developmental genes required for skeletogenesis (*Lmo4*, *Runx2*, *Sp7*, members of the *Lef1/Tcf* family, *Col1a1*, *Alpl*, *Bmpr1a*, *Fgfr3*, *Wnt5a*, *Tgfb2* and others) (Supplemental Fig. 1 and Supplemental Table 1), we

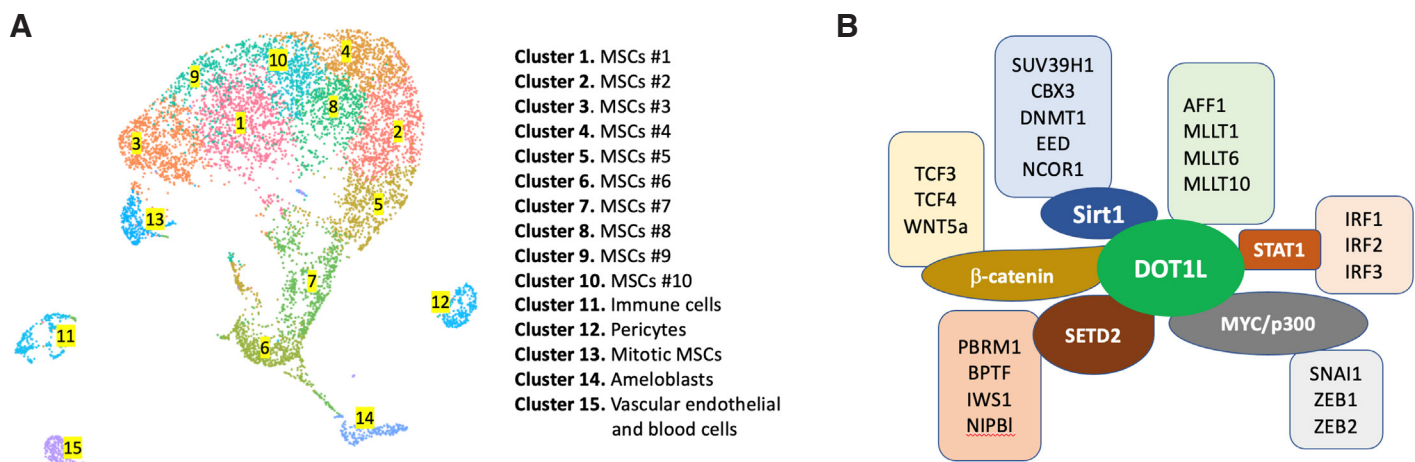


**Fig. 1. scRNA-seq clustering analysis of the mouse molar dental pulp.** (A) The mouse molar dental pulp is composed of 15 distinct cell types that represent MSCs at different stages of osteogenic and odontogenic differentiation as well as pericytes, ameloblasts, immune cells and vascular endothelial cells. (B) STRING interaction network analysis revealed that Dot1L associates with SIRT1, SETD2, the MYC/p300 regulatory axis and  $\beta$ -catenin. SIRT1 physically interacts with SUV39H1, CBX3, DNMT1, NCOR1 and EED, key components of the repressive chromatin complexes. By contrast, SETD2 interacts with PBRM1, BPTF, NIPBL and IWS1, which are associated with transcriptional activation. The MYC/p300 regulatory axis controls the expression of *Snai1*, *Zeb1* and *Zeb2*. Dot1L interacts with  $\beta$ -catenin, which regulates the expression of the WNT signaling genes *Tcf3*, *Tcf4* and *Wnt5a*.

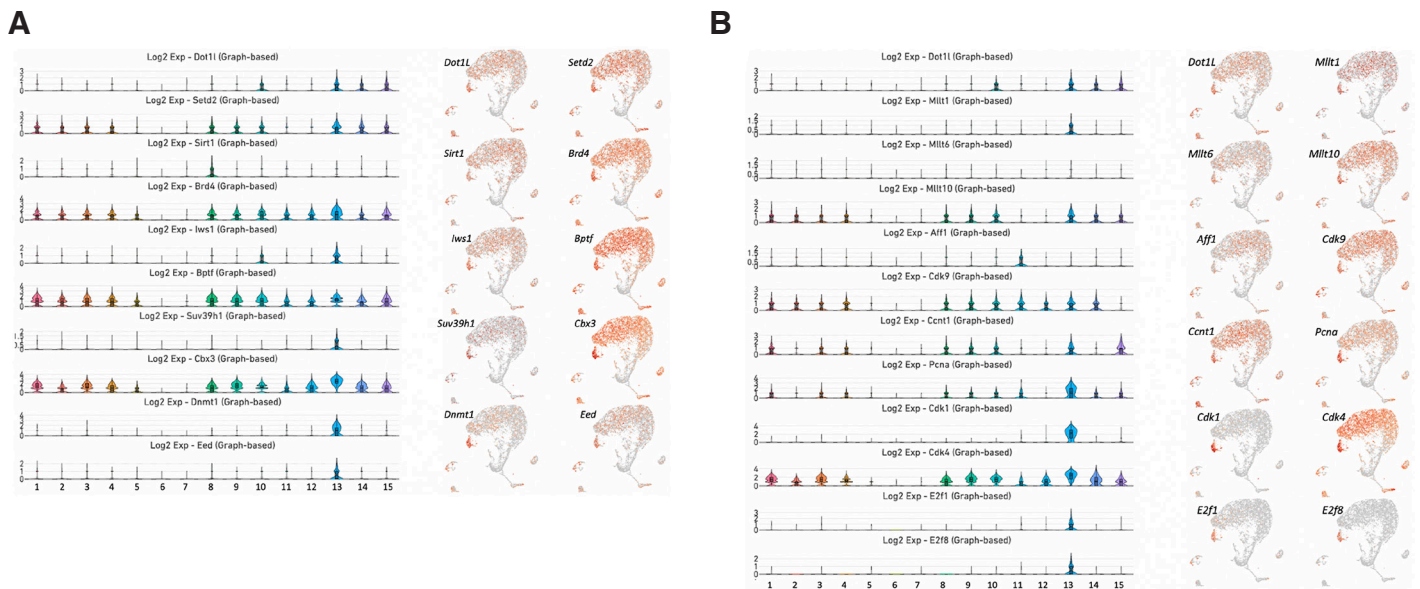


**Fig. 2. Expression of genes encoding epigenetic interactors, transcription elongation factors and downstream targets of Dot1L.** (A) Violin plots of the genes *Dot1L*, *Setd2*, *Sirt1*, *Brd4*, *Iws1*, *Bptf*, *Suv39h1*, *Cbx3*, *Dnmt1* and *Eed* (left). UMAP visualization of genes encoding the components of the transcription activation complex, proteins involved in DNA methylation and components of the PRC2 (right). (B) Violin plots of the genes *Dot1L*, *Mllt1*, *Mllt6*, *Mllt10*, *Aff1*, *Cctn1*, *PcnA*, *Cdk1*, *Cdk4*, *Cdk9*, *E2f1* and *E2f8* (left). UMAP visualization of genes encoding proteins involved in transcription elongation and cell cycle progression (right).

identified 11 clusters of MSCs referred to as MSCs #1 to #10 and #13. Tooth development relies on reciprocal interactions between the ectoderm-derived dental epithelium and the underlying neural crest (NC)-originated mesenchyme (Hermans *et al.*, 2021). In the mouse dental pulp, MSCs are derived from the cranial NC. A selective group of transcription factors known as NC master regulators, including *Dlx*, *Msx*, *Sox*, *Id*, *Snai*, *Twist* and others, control the NC specification program (Simoes-Costa and Bronner, 2015). We found that *Dlx5*, *Twist1*, *Msx1*, *Msx2*, *Sox9* and members of the *Id* family are broadly expressed in all 11 subpopulations of MSCs (Supplemental Fig. 2).

Although previous reports have demonstrated that the dental pulp is composed of both fibroblasts and MSCs (Alvarez-Vasquez *et al.*, 2022; Mollentze *et al.*, 2021), we use MSCs as a common name to define both cell types. Recent studies have shown that MSCs and fibroblasts are identical with respect to their proliferation and differentiation capacities, gene expression profiles and immunomodulatory properties (Hematti, 2012; Denu *et al.*, 2016; Soundararajan and Kannan, 2018), and it has been proposed that fibroblasts are in fact aged MSCs. Moreover, recent scRNA-seq studies have revealed significant similarities between cell subsets derived from MSCs and fibroblasts based on comprehensive analyses of integrated single-cell transcriptome data (Fan *et al.*, 2022; Soliman *et al.*, 2021). The authors suggested that MSCs represent a subclass of fibroblasts.

Differential expression of the osteogenic genes *Lef1*, *Tcf7*, *Runx2*, *Sp7*, *Sp1*, *Snai1*, *Snai2*, *Twist2*, *Lmo4*, *Cebpb* and *Myc*, which encode transcription factors, suggests that clusters 1 to 5 and 8 to 10 represent subpopulations of MSCs undergoing different phases of osteogenic differentiation. These clusters are also enriched in genes essential for skeletal development such as *Alpl*, *Col1a1*, *Fgfr3*, *Wnt5a* and *Tgfb2* (Supplemental Fig. 1). Cluster 6 contains an undifferentiated population of stromal cells characterized by

expression of *Slc40a1*, *Cd55*, *Col3a1*, *Col5a2* and *Col9a2* (Supplemental Table 1). In the adjacent cluster 7, we observed relatively modest expression of *Alp*, *Col3a1*, *Fgfr1*, *Satb2*, *Id1*, *Id2* and *Tgfb2* (Supplemental Fig. 1 and Supplemental Table 1). Within clusters 3 and 7, we identified a subpopulation of odontogenic cells enriched in *Bglap*, *Dspp* and *Dmp1* (Supplemental Fig. 3).

There are some challenges to labeling stem cells in dental tissues using well-accepted markers such as *Plp1* (Kaukua *et al.*, 2014), *Ng2/Cspg4* (Iwasaki *et al.*, 2013), *Gli1* (Zhao *et al.*, 2014) and *Sox2* (Sanz-Navarro *et al.*, 2018). Although these markers are frequently used to trace stem cells, researchers have observed the expression of these genes in many tissues and cell types; more importantly, these markers are nearly ubiquitously expressed in skeletal lineages at different developmental stages (Ambrosi *et al.*, 2019). Thus, based on the expression profiles of *Plp1*, *Cspg4*, *Gli1* and *Sox2*, we cannot pinpoint a specific cluster as a population that represents stem cells, although the data hint that cluster 3 is likely to harbor a population of stem cells (Supplemental Fig. 4). Further research based on lineage tracing is required to define these cells.

Cluster 11 represents immune cells and is enriched in *Fcer1g*, *Tyrobp*, *C1qb*, *Csf1r* and *Pf4* (Supplemental Fig. 5 and Supplemental Table 1). Cluster 12 defined pericytes, which express *Rgs5*, *Ndufa4l2*, *Casq2*, *Acta2* and *Myh11* (Supplemental Fig. 6 and Supplemental Table 1). We found that cluster 13 is enriched in a highly proliferative population of MSCs, as evidenced by an enrichment of genes involved in cell division or DNA replication (i.e., *Nusap1*, *Spc25*, *Pimreg*, *Cenpf* and *Birc5*) (Supplemental Fig. 7 and Supplemental Table 1). Cluster 14 represents ameloblasts based on the expressions of *Krt5*, *Amelx*, *Fxyd3*, *Mmp20* and *Enam* (Supplemental Fig. 8 and Supplemental Table 1), whereas cluster 15 exhibits transcriptional profiles compatible with vascular endothelial cells (i.e., enrichment in *Cdh5*, *Plvap*, *Ctla2a*, *Emcn* and *Cldn5*) (Supplemental Fig. 9 and Supplemental Table 1).

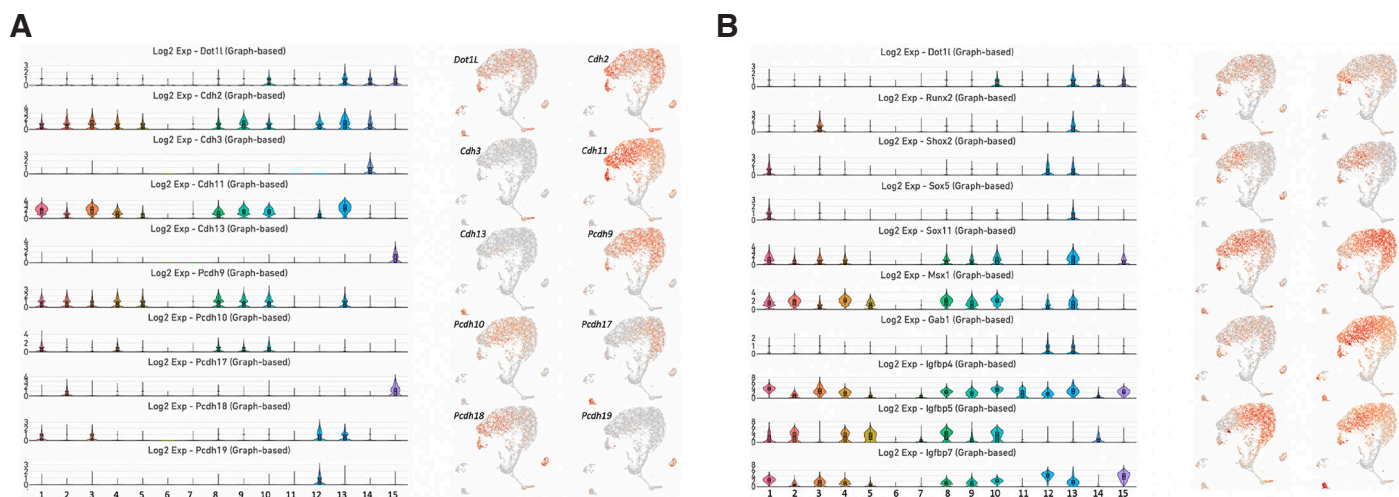


**Fig. 3. Expression of genes encoding cadherins, protocadherins, osteogenic transcription factors and members of the IGF signaling pathway. (A)** Violin plots of the genes *Cdh2*, *Cdh3*, *Cdh11*, *Cdh13*, *Pcdh9*, *Pcdh10*, *Pcdh17*, *Pcdh18* and *Pcdh19* (left). UMAP visualization of genes encoding proteins involved in cell adhesion and cell-cell signaling (right). **(B)** Violin plots of the genes *Runx2*, *Shox2*, *Sox5*, *Sox11*, *Mx1*, *Gab1*, *Igfbp4*, *Igfbp5* and *Igfbp7* (left). UMAP visualization of these genes (right).

### Expression of *Dot1L* and epigenetic factors associated with *Dot1L* in the mouse molar dental pulp

The histone methyltransferase *Dot1L* regulates transcriptional initiation and elongation by recruiting RNA polymerase II to unmethylated CpG-rich promoters by forming a functional complex with different cofactors (Miyamoto et al., 2020). Protein interaction networks are critical for a system-level epigenetic understanding of gene regulatory processes. By analyzing the STRING interaction network (<https://string-db.org>), we discovered that *Dot1L* has a specific set of interacting partners (Fig. 1B). We identified SIRT1 and SETD2 as interacting partners of *Dot1L*. Our STRING analysis revealed that EED, a key component of the polycomb repressive complex 2 (PRC2), and the repressive proteins SUV39H1, CBX3 and DNMT1, which are known to be associated with heterochromatin and DNA methylation (Weirich et al., 2021; van Wijnen et al., 2021; Qin et al., 2011), can physically interact with SIRT1. In addition, *Dot1L* cooperates with the c-MYC-p300 complex to activate regulators of the epithelial-mesenchymal transition (Cho et al., 2015). The interaction of *DOT1L* with  $\beta$ -catenin and STAT1 ensures the proper control of the downstream targets of the WNT and JAK-STAT pathways (Monteagudo et al., 2017; Shah and Henriksen, 2011). Interestingly, although our uniform manifold approximation and projection (UMAP) analysis showed that *Dot1L* is broadly expressed in most clusters within the molar dental pulp, the violin plots clearly demonstrated an enrichment of *Dot1L* in clusters 10, 13, 14 and 15 (Fig. 2 and Supplemental Fig. 10). Next, we analyzed the expression of genes encoding critical protein partners of *Dot1L*. *Setd2* was enriched in clusters 1, 2, 3, 4, 8, 9, 10, 13, 14 and 15. *Sirt1* exhibited a more restricted expression with enrichment in cluster 8, while *Suv39h1*, *Dnmt1* and *Eed* were mainly expressed in cluster 13 representing mitotic MSCs. *Brd4*, *Bptf* and *Cbx* were abundantly expressed in clusters 1, 2, 3, 4, 5, 8, 9, 10, 11, 12, 13, 14 and 15 (Fig. 2A and Supplemental Figs. 10 and 11). *Dot1L* participates in transcriptional elongation by forming a complex with AFF1, MLLT1, MLLT6 and MLLT10. We analyzed the expression pattern of genes encoding these factors. We detected

expression of *Mllt10* in clusters 1, 2, 3, 4, 8, 9, 10, 13, 14 and 15 (Fig. 2B and Supplemental Fig. 12). By contrast, *Mllt1* was weakly expressed in many clusters although we observed some elevated expression in cluster 13. *Mllt6* and *Aff1* displayed relatively weak expression in all clusters.

### Expression of downstream targets of *Dot1L* associated with cell cycle progression

Prior studies in erythroid progenitors, lung cells and chondrocytes reported that *Dot1L* loss of function induced decreased expression of genes involved in cell cycle regulation and proliferation (Kim et al., 2014; Sutter et al., 2021). Thus, we analyzed the expression profiles of cell cycle genes that are known downstream targets of *Dot1L* (Sutter et al., 2021). We found robust expression of *Cdk4* and *Cdk9* in clusters 1, 2, 3, 4, 8, 9, 10, 11, 12, 13 and 14 (Fig. 2B and Supplemental Figs. 12 and 13). In addition, *Cdk4* was actively expressed in cluster 15. By contrast, expression of *Cdk1*, *E2f1* and *E2f8* was limited to cluster 13. *Ccnt1* was enriched in clusters 1, 3, 4, 8, 9, 10, 13 and 15. *Pcna* exhibited a similar expression pattern with enrichment in clusters 1, 3, 4, 8, 9, 10, 11, 13, 14 and 15 (Fig. 2B and Supplemental Fig. 12).

### Expression of cadherin and protocadherin genes, known downstream targets of *Dot1L*

Research indicates that depletion of *Dot1L* in *Prrx1*-expressing limb progenitors leads to dysregulation of cadherin and protocadherin genes (Sutter et al., 2021). Cadherin and protocadherin are at the crossroads of different signaling pathways (Pancho et al., 2020). Therefore, we performed a careful analysis of the expression profiles of these subfamilies in the mouse dental pulp. We found high levels of expression of *Cdh2* and *Cdh11* in clusters 1, 2, 3, 4, 5, 8, 9, 10, 12 and 13 (Fig. 3A). In addition, *Cdk2* was expressed in cluster 14. By contrast, expression of *Cdh3* and *Cdh13* was limited to cluster 14 and cluster 15, respectively. *Pcdh9* was enriched in clusters 1, 2, 3, 4, 5, 8, 9, 10 and 13. *Pcdh10* was expressed in clusters 1, 4, 8, 9 and 10. Expression of *Pcdh18* was limited to

clusters 2 and 15. *Pcdh18* was expressed in clusters 1, 3, 12 and 13, whereas *Pcdh19* was restricted to cluster 12 (Fig. 3A).

### Expression of *Dot1L* transcriptional targets and downstream regulated pathways

We analyzed the expression profiles of genes encoding members of the IGF signaling pathway and some key transcription factors that were previously reported to be downstream targets of *Dot1L* in mouse limb chondrocytes (Sutter *et al.*, 2021). The expression of *Runx2* was limited to clusters 3 and 13 (Fig. 3B). *Shox2* was expressed in clusters 1, 12 and 13, while *Sox5* expression was restricted to clusters 1 and 13. By contrast, *Sox11* displayed vigorous expression in clusters 1, 2, 3, 4, 8, 9, 10, 13, 14 and 15. Similarly, *Msx1* was strongly expressed in clusters 1, 2, 3, 4, 5, 8, 9, 10, 13, 14 and 15. We identified high levels of *Igfbp4* expression in clusters 1, 2, 3, 4, 5, 7, 8, 9, 10, 11, 12, 13, 14 and 15. *Igfbp5* was expressed in clusters 1, 2, 4, 5, 7, 8, 9, 10 and 14, whereas *Igfbp7* was more broadly expressed in clusters 1, 2, 3, 4, 5, 8, 9, 10, 12, 13 and 15 (Fig. 3B).

*Ctnnb1* encoding  $\beta$ -catenin displayed a broad range of expression in the molar dental pulp (Fig. 4A). With the exception of clusters 6 and 7, *Ctnnb1* was expressed in all other subpopulations of MSCs, as well as immune cells (cluster 11), pericytes (cluster 12), ameloblasts (cluster 14) and vascular endothelial cells (cluster 15). However, genes encoding transcription factors and ligands of the WNT signaling pathway exhibited a more restricted expression pattern. We noticed vigorous expression of *Lef1*, *Tcf3*, *Tcf4*, *Tcf7*, *Wnt5a*, *Wnt6* and *Wnt10a* in cluster 13 (Fig. 4A). By contrast, expression of *Tcf3*, *Tcf4* and *Wnt5a* was limited to cluster 10. The *Tle1* gene, which encodes a member of the TLE/Groucho family of transcriptional corepressors, was mainly enriched in cluster 12 (pericytes).

Analysis of the expression patterns of the downstream targets of the *Myc/p300* regulatory axis and JAK-STAT signaling pathway revealed enrichment of *Ep300*, *Snai1*, *Zeb1* and *Zeb2* in clusters 10 and 13, whereas *c-Myc* was enriched in cluster 10 only (Fig. 4B). *Stat1* and transcription factors *Irf1*, *Irf2* and *Irf3* associated with the JAK-STAT pathway were actively expressed in clusters 10 and 13.

### DNA demethylation, chromatin accessibility and RNA expression of *Dot1L*

We examined the genomic structure of *Dot1L* for the DNA demethylation mark 5-hydroxymethylcytosine (5hmC) and chromatin accessibility. 5hmC and open chromatin are hallmark features of genes that are actively transcribed. Using RNA-seq, assay for transposase-accessible chromatin using sequencing (ATAC-seq) and hydroxymethylated DNA immunoprecipitation sequencing (hMeDIP-seq) assays, we previously determined gene expression, accessible chromatin regions and genome-wide enrichment of 5hmC in the mouse dental pulp (Joshi *et al.*, 2022a; Joshi *et al.*, 2022b). By analyzing these datasets, we found that the genomic region across actively transcribed *Dot1L* gene exhibited open chromatin enriched in 5hmC (Fig. 5). Collectively, our results suggest that the *Dot1L* locus acquired an active chromatin state in the mouse dental pulp.

### Discussion

In the current study, we investigated the expression profile of *Dot1L* in the mouse molar dental pulp. Within 15 clusters of cells that represent pericytes, ameloblasts, vascular endothelial cells and MSCs, we found that *Dot1L* is significantly enriched in two subpopulations of MSCs at different stages of osteogenic differentiation (clusters 10 and 13), as well as in ameloblasts (cluster 14) and vascular endothelial cells (cluster 15).

We further investigated the expression patterns of components of the transcription initiation and elongation complexes associated with *Dot1L* in the mouse molar dental pulp. We identified a core set of genes that are common in these two clusters (Fig. 6). These genes encode SETD2, BRD4, IWS1, BPTF and MLLT10, which are key components of the transcription initiation and transcription elongation complexes. The mouse STRING database revealed that SIRT1 also interacts with EED, which is a subunit of the PRC2. In addition, SIRT1 forms a complex with factors involved in DNA methylation such as CBX3 and DNMT1. We analyzed the expression patterns of *Eed*, *Cbx3* and *Dnmt1* in the molar dental pulp and found that *Cbx3* was expressed in both clusters, whereas *Eed* and

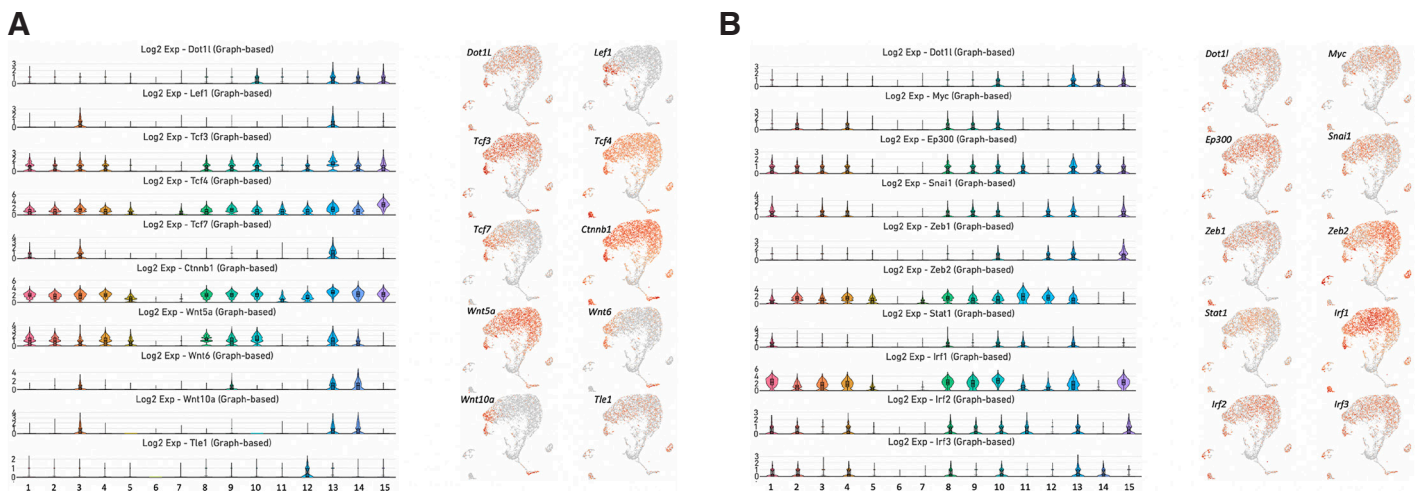


**Fig. 4. Expression of genes encoding members of the WNT signaling pathway and the MYC/p300 regulatory axis. (A)** Violin plots of the genes *Lef1*, *Tcf3*, *Tcf4*, *Tcf7*, *Ctnnb1*, *Wnt5a*, *Wnt6*, *Wnt10a* and *Tle1* (left). UMAP visualization of these genes (right). **(B)** Violin plots of the genes *Myc*, *p300*, *Snai1*, *Zeb1*, *Zeb2*, *Stat1*, *Irf1*, *Irf2* and *Irf3* (left). UMAP visualization of these genes (right).

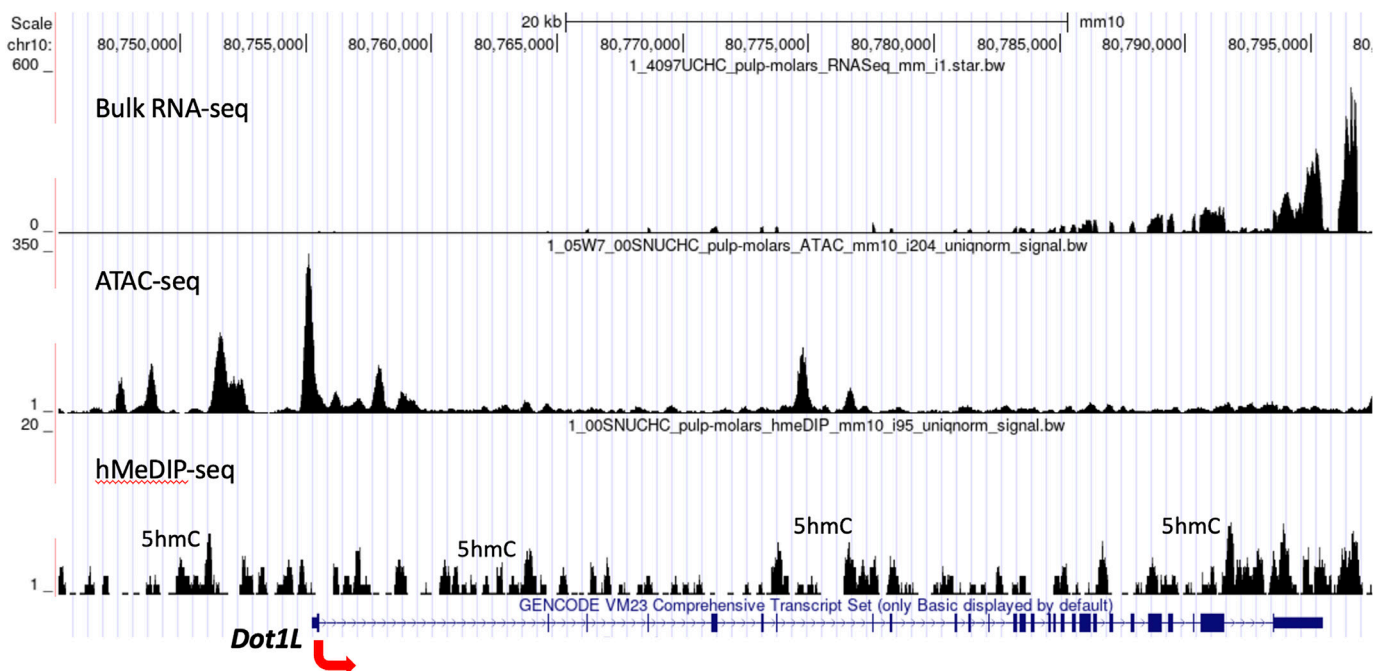


**Fig. 5. Chromatin organization of *Dot1L* in the mouse molar dental pulp.** The genomic landscape of *Dot1L* in the mouse molar dental pulp. The hMeDIP-seq peaks are high in the promoter and gene body regions, indicating that 5hmC is enriched in the *Dot1L* locus. Strong ATAC-seq peaks are present in the transcription start site and promoter, which correlates with robust expression of *Dot1L* in the dental pulp.

*Dnmt1* exhibited vigorous expression in cluster 13. Interestingly, cluster 13 represented mitotic MSCs that undergo cell division. The core set of transcription factors that were enriched in this subpopulation include *Runx2*, *Shox2*, *E2F1*, *E2F8* and *Sox5*.

Surprisingly, *Dot1L* was not expressed uniformly across all identified MSCs (clusters 1–10 and 13). Some minor enrichment of *Dot1L* in the proliferating MSCs (cluster 13) within the mouse molar dental pulp is consistent with reports that *Dot1L* balances cell proliferation and differentiation by preventing premature cell cycle exit in progenitor populations (Nguyen and Zhang, 2011; Kim et al., 2014; Franz et al., 2019; Aslam et al., 2021). Although a major function of *Dot1L* is linked to cell proliferation (McLean et al., 2014), the impact of *Dot1L* depletion varies depending on the cell type or developmental stage (Kim et al., 2014). In previous studies, we showed that loss of *Dot1L* function in chondrocytes impaired transcriptional regulation of multiple genes implicated in cell cycle control and the IGF signaling pathway (Sutter et al., 2021). Our single-cell transcriptome analysis showed that *Cdk4*, *Cdk9*, *Ccnt1*, *Pcna*, *Cdh2*, *Cdh11*, *Pcdh9*, *Igfbp4* and *Igfbp7* were among the common genes enriched in clusters 10 and 13.

The expression of *Dot1L* in cluster 15 within the molar dental pulp is also congruent with published studies showing a mechanistic role for *Dot1L* in the development of the vasculature (Duan et al., 2016). Specifically, Duan et al., reported that *Dot1L* cooperates with the transcription factor *ETS-1* to stimulate the expression of *VEGFR2*, thereby activating the ERK1/2 and AKT signaling pathways and promoting angiogenesis.

*Dot1L* is the only mammalian histone methyltransferase that catalyzes H3K79 methylation to mediate transcriptional activation (Vlaming and Leeuwen, 2016). *Dot1L* interacts with AF10, AF17 and ENL to regulate transcriptional elongation. Recent research

showed that *Dot1L* is also involved in transcription initiation (Wu et al., 2021). Surprisingly, depletion of *Dot1L* and ENL reduced occupancy of the TATA-binding protein TBP and RNA polymerase II along target genes. Researchers have proposed that *Dot1L* may regulate transcription initiation by facilitating the recruitment of the transcription factor IID (Wu et al., 2021).

With the assistance of the histone H3K27 acetyltransferases CBP and p300, *Dot1L* is involved in sustaining cell-type-specific gene expression (Ebrahimi et al., 2019). H3K79 methylation mediated by *Dot1L* controls enhancer-promoter interactions and activation of specific marker genes in leukemia cells (Godfrey et al., 2021). However, during B-cell differentiation, *Dot1L* supports the repression of PRC2 targets associated with an antiproliferative plasma cell differentiation program (Aslam et al., 2021). Pharmacologic inhibition of *Dot1L* synergizes with the loss of SETD2 to induce growth arrest, DNA damage, differentiation and cell death (Skucha et al., 2018). *Dot1L* forms a complex with MLLT10/AF10 to bind TCF4/ $\beta$ -catenin in mouse small intestinal crypts (Mahmoudi et al., 2010). The recruitment of the MLLT10/AF10-*Dot1L* complex in a  $\beta$ -catenin-dependent manner results in H3K79 methylation and transcriptional elongation of WNT target genes. Surprisingly, *Dot1L* is also implicated in heterochromatin formation. Mouse embryonic stem cells (ESCs) deficient for *Dot1L* exhibit loss of H3K79 methylation accompanied by reduced heterochromatin marks H3K9me2 and H4K20me3, leading to proliferation defects, telomere elongation and aneuploidy (Jones et al., 2008).

While methylation of H3K79 is viewed as the sole molecular function of *Dot1L* activity, recent studies support methyltransferase-independent functions of *Dot1L* in ESCs, including transcriptional elongation and cellular differentiation (Cao et al., 2020). The global loss of *Dot1L* in mouse embryos firmly established the essential

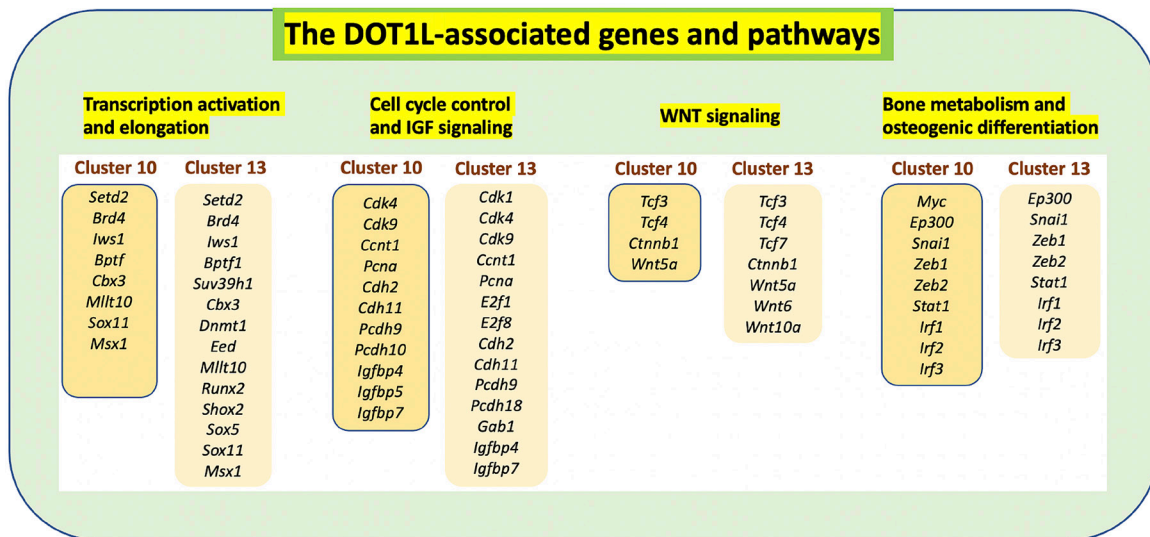


**Fig. 6. Dot1L-associated genes and signaling pathways.** *Dot1L* is primarily expressed in clusters 10 and 13 representing MSCs at different stages of osteogenic differentiation. *Dot1L* associates with other components of transcription initiation and elongation to control the cell cycle and the expression of downstream targets of the WNT and IGF signaling pathways.

role of *Dot1L* in mammalian erythropoiesis (Feng *et al.*, 2010), yet *in vivo* studies using a novel *Dot1L* methyltransferase mutant mouse model provided compelling evidence that *Dot1L*-controlled early embryonic erythropoiesis is independent of its intrinsic H3K79 methyltransferase activity (Malcom *et al.*, 2022). These observations provide a strong rationale to thoroughly examine the functional contributions of *Dot1L* catalytic versus non-catalytic activities within various developmental processes and tissues, including the dental pulp. Some of the regulatory functions of *Dot1L* are likely mediated through its interactions with lineage-specific transcription factors or other chromatin remodeling complexes.

Our study revealed that *Dot1L* colocalizes with genes encoding protein interactors involved in epigenetic activation such as *Setd2*, *Sirt1*, *Brd4*, *Isw1*, *Bptf* and *Suv39h1*. In addition, we found that *Dot1L* is co-expressed with *Eed2*, *Cbx3* and *Dnmt1*, which encode epigenetic factors associated with gene silencing and heterochromatin formation. Furthermore, we found that *Dot1L* is co-expressed with downstream targets of the IGF and WNT signaling pathways and cell cycle progression. Therefore, our findings suggest that *Dot1L* plays an important role in orchestrating lineage-specific gene expression during the differentiation of MSCs.

Collectively, our scRNA-seq analysis unmasked population heterogeneity of the mouse molar dental pulp. More importantly, our study provided invaluable insight into the single-cell gene expression pattern of *Dot1L* in osteogenic and odontogenic progenitors. Further investigation toward identifying the molecular pathways through which *Dot1L* histone methyltransferase orchestrates gene regulation will provide a more refined understanding of the fundamental mechanisms underlying the development of dental structures.

## Materials and Methods

### scRNA-seq and data analysis

We prepared primary pulp from the molars of 5- to 6-day-old mice according to previously described procedures (Balic *et al.*, 2010). Viability of each single-cell suspension was assessed using

a Countess II FL Automated Cell Counter (Thermo Fisher Scientific Inc., Waltham, MA). Suspensions of dissociated cells were loaded onto independent single channels of a Chromium Controller (10× Genomics, Pleasanton, CA) single-cell platform. Briefly, we loaded ~8,112 single cells for capture using a Chromium Single Cell 3' Reagent kit, v2 Chemistry (10× Genomics). Following capture and lysis, complementary DNA was synthesized and amplified (14 cycles) as per the 10× Genomics protocol. The amplified cDNA was used to construct an Illumina sequencing library and was sequenced on a single lane of a HiSeq 4000 (Illumina, San Diego, CA).

### Genome-wide ATAC-seq, hMeDIP-seq and RNA-seq

ATAC-seq, hMeDIP-seq and RNA-seq services were performed by Active Motif (Carlsbad, CA). RNA isolation was performed using the RNAeasy Mini/Midi kit (Qiagen, Germantown, MD). RNA-seq was performed using an Illumina NextSeq 500 to generate 42-nt paired-end sequences. For ATAC-seq and RNA-seq, the paired-end 42-bp sequencing reads generated by Illumina NextSeq 500 sequencing were mapped to the genome using the Burrows-Wheeler aligner (BWA) algorithm with default settings. For hMeDIP-seq, genomic DNA was isolated using the Monarch Genomic DNA Purification kit (New England Biolabs, Ipswich, MA) following the manufacturer's instructions. DNA was sonicated to ~150–300 bp and Illumina adaptors were ligated to the DNA ends. To generate genome-wide maps of 5hmC, Active Motif performed hMeDIP-seq experiments using the antibody AM39791 to 5hmC. The input DNA was used as a control. Finally, immunoprecipitated DNA and input DNA that did not go through the immunoprecipitation step were processed into sequencing libraries and sequenced using the Illumina platform (NextSeq 500, 75-nt single-end).

### Computational analysis

#### scRNA-seq

Analysis of scRNA-seq was completed using mouse molar dental pulp labeled as BD19002. The target was 6,000 cells, which

produced an estimated 8,735 cells with 44,363 average reads per cell. Overall, the analysis utilized scanpy (Wolf *et al.*, 2018), comprising several steps as detailed below. Quality control for the scRNA-seq FASTQ reads included:

- (1) filtering FASTQ reads with more than 1 bp mismatched barcode (10X Genomics, 2018)
- (2) filtering FASTQ reads with less than a 3 Q30 score
- (3) filtering STAR alignments with less than a 255 MAPQ score (Dobin *et al.*, 2013)

Samples were processed independently and then batch corrected via the BBKNN method (Polański *et al.*, 2020). Single-cell clustering procedures do not perfectly partition cell types, but instead indicate similarity of expression patterns which can be useful for exploring specific gene profiles of genes such as *Dot1L*. The isolated cluster expression patterns can then be associated with cell mixtures by using cell-specific markers previously documented in the literature. Here, prior expression profiles derived from the 3,500 most variable dispersed genes were used to calculate the local neighborhood of the cells (Satija *et al.*, 2015; Zheng *et al.*, 2017). Next, a neighborhood graph was generated using the k-nearest neighbors (for k=30) algorithm, followed by dimensional reduction using the UMAP procedure (Becht *et al.*, 2018). The neighborhood graph was then batch corrected with BBKNN (Polański *et al.*, 2020). Single-cell clusters were assigned in the UMAP space according to the Leiden community detection method (Tragg *et al.*, 2019). In addition to the above scanpy analysis, single-cell subclusters were generated visually when not automatically detected using the web-based Cellview software, which provides interactive viewing of the downstream data (Bolisetty *et al.*, 2017). Figures generated for this work made use of screen captures of the Cellview interactions and supported the numerical results.

#### ATAC-seq

Genomic regions with high levels of ATAC-seq transposition/tagging events were determined using the MACS2 peak-calling algorithm (Zhang *et al.*, 2008). Since both reads (tags) from paired-end sequencing represent transposition events, both were used for peak-calling but were treated as single, independent reads. To identify the density of the transposition events along the genome, the genome was divided into 32-bp bins and the number of fragments in each bin was determined. For this purpose, the reads were extended to 200 bp, which is close to the average length of the sequenced library inserts. In the default analysis, the tag number of all samples was reduced (by random sampling) to the number of tags present in the smallest sample. To compare peak metrics between two or more samples, overlapping intervals were grouped into “merged regions,” which were defined by the start coordinate of the most upstream interval and the end coordinate of the most downstream interval (to determine the union of overlapping intervals). In locations unique to a sample, the merged region was assigned to the interval. After defining the intervals and merged regions, the genomic locations and features were summarized and presented in Excel spreadsheets.

#### hMeDIP-seq

hMeDIP-seq reads were mapped to the mouse genome (mm10) using the BWA algorithm with default settings. Alignment information for each read was stored in the BAM format. For the analysis, only uniquely mapped reads without duplicates were used, and

tag numbers were normalized to the lowest number among the samples (by downsampling), which was 19.7 million. Methylated regions (peak intervals) were identified using the MACS2 peak-calling algorithm (Zhang *et al.*, 2008) with a default cutoff of p-value = 1e-7. The 5hmC tag distributions around the genes were determined and presented as average plots (average of values for all target regions).

#### Bulk RNA-seq

The 42 bp-long read-pair bulk RNA-seq fragments were mapped to the reference genome mm10 using the STAR aligner (Dobin *et al.*, 2013). A fragment assignment step was carried out to count the number of fragments overlapping the genomic sequence. Only the read pairs that had both ends aligned at the same chromosome and the same DNA strand were considered for subsequent analyses. Feature counts (FPKM assignment to genes) were performed using the Subread package (Liao *et al.*, 2014). Gene annotations were originally from the NCBI RefSeq database and then adapted by merging the overlapping exons from the same gene to form a set of disjoint exons for each gene. After obtaining the same table containing the fragments (or reads) of genes, differential analysis was performed using DESeq2 (Love *et al.*, 2014).

#### Acknowledgments

This project was funded by the grant REP-401754-20144-20 from the University of Connecticut to DB. We thank all members of the MM, RG and DB laboratories. The data that support the findings of this study are available on request.

#### Author contributions

DB: conceptualization. AV, BE and PR: methodology. DB, RG, TB, BE and PJ: data analysis. DB, PR and MM: reagents and materials. DB, RG, BE and TB: writing. DB, MM and DG: supervision. DB: funding acquisition. All authors gave final approval and agreed to be accountable for all aspects of the work.

#### References

- ÁLVAREZ-VÁSQUEZ J. L., CASTAÑEDA-ALVARADO C. P. (2022). Dental Pulp Fibroblast: A Star Cell. *Journal of Endodontics* 48: 1005-1019. <https://doi.org/10.1016/j.joen.2022.05.004>
- AMBROSI T. H., LONGAKER M. T., CHAN C. K. F. (2019). A Revised Perspective of Skeletal Stem Cell Biology. *Frontiers in Cell and Developmental Biology* 7: 189. <https://doi.org/10.3389/fcell.2019.00189>
- ASLAM M. A., ALEMDEHY M. F., KWESI-MALIEPAARD E. M., MUHAJIMIN F. I., CAGANOVA M., PARDIECK I. N., BRAND T., WELSEM T., RINK I., SONG J.Y., WIT E., ARENS R., JACOBS H., LEEUWEN F. (2021). Histone methyltransferase DOT1L controls state-specific identity during B cell differentiation. *EMBO reports* 22: e51184. <https://doi.org/10.15252/embr.202051184>
- BALIC A., AGUILA H. L., CAIMANO M. J., FRANCONI V. P., MINA M. (2010). Characterization of stem and progenitor cells in the dental pulp of erupted and unerupted murine molars. *Bone* 46: 1639-1651. <https://doi.org/10.1016/j.bone.2010.02.019>
- BARRY E. R., KRUEGER W., JAKUBA C. M., VEILLEUX E., AMBROSI D. J., NELSON C. E., RASMUSSEN T. P. (2009). ES Cell Cycle Progression and Differentiation Require the Action of the Histone Methyltransferase Dot1L. *Stem Cells* 27: 1538-1547. <https://doi.org/10.1002/stem.86>
- BAYARSAIHAN D., ENKHMANDAKH B., VIJAYKUMAR A., ROBSON P., MINA M. (2022). Single-cell transcriptome analysis defines mesenchymal stromal cells in the mouse incisor dental pulp. *Gene Expression Patterns* 43: 119228. <https://doi.org/10.1016/j.gep.2021.119228>
- BECHTE, MCINNES L., HEALY J., DUTERTRE C. A., KWOK I. W. H., NGL. G., GINHOUX F., NEWELL E. W. (2018). Dimensionality reduction for visualizing single-cell data using UMAP. *Nature Biotechnology* 37: 38-44. <https://doi.org/10.1038/nbt.4314>

- BOLISETTY MOHAN T., STITZEL MICHAEL L., ROBSON PAUL (2017). CellView: Interactive exploration of high dimensional single cell RNA-seq data. *bioRxiv.org* : Preprint 123810. <https://doi.org/10.1101/123810>
- BOVIO P. P., FRANZ H., HEIDRICH S., RAULEAC T., KILPERT F., MANKE T., VOGEL T. (2019). Differential Methylation of H3K79 Reveals DOT1L Target Genes and Function in the Cerebellum In Vivo. *Molecular Neurobiology* 56: 4273-4287. <https://doi.org/10.1007/s12035-018-1377-1>
- CAO K., UGARENKO M., OZARK P. A., WANG J., MARSHALL S. A., RENDLEMAN E. J., LIANG K., WANG L., ZOU L., SMITH E. R., YUE F., SHILATIFARD A. (2020). DOT1L-controlled cell-fate determination and transcription elongation are independent of H3K79 methylation. *Proceedings of the National Academy of Sciences* 117: 27365-27373. <https://doi.org/10.1073/pnas.2001075117>
- CHO M.H., PARK J.H., CHOI H.J., PARK M.K., WON H.Y., PARK Y.J., LEE C. H., OH S.H., SONG Y.S., KIM H. S., OH Y.H., LEE J.Y., KONG G. (2015). DOT1L cooperates with the c-Myc-p300 complex to epigenetically derepress CDH1 transcription factors in breast cancer progression. *Nature Communications* 6: 7821. <https://doi.org/10.1038/ncomms8821>
- DENU R. A., NEMCEK S., BLOOM D. D., GOODRICH A. D., KIM J., MOSHER D. F., HEMATTI P. (2016). Fibroblasts and Mesenchymal Stromal/Stem Cells Are Phenotypically Indistinguishable. *Acta Haematologica* 136: 85-97. <https://doi.org/10.1159/000445096>
- DOBINA A., DAVIS C. A., SCHLESINGER F., DRENKOW J., ZALESKI C., JHA S., BATUT P., CHAISSON M., GINGERAS T. R. (2013). STAR: ultrafast universal RNA-seq aligner. *Bioinformatics* 29: 15-21. <https://doi.org/10.1093/bioinformatics/bts635>
- DUAN Y., WU X., ZHAO Q., GAO J., HUO D., LIU X., YE Z., DONG X., FU Z., SHANG Y., XUAN C. (2016). DOT1L promotes angiogenesis through cooperative regulation of VEGFR2 with ETS-1. *Oncotarget* 7: 69674-69687. <https://doi.org/10.18632/oncotarget.11939>
- EBRAHIMIA., SEVINÇ K., GÜRHAN SEVINÇ G., CRIBBS A. P., PHILPOTT M., UYULUR F., MOROVA T., DUNFORD J. E., GÖKLEMEZ S., ARI SULE, OPPERMANN U., ÖNDER T. T. (2019). Bromodomain inhibition of the coactivators CBP/EP300 facilitate cellular reprogramming. *Nature Chemical Biology* 15: 519-528. <https://doi.org/10.1038/s41589-019-0264-z>
- FAN C., LIAO M., XIE L., HUANG L., LV S., CAI S., SU X., WANG Y., WANG H., WANG M., LIU Y., WANG Y., GUO H., YANG H., LIU Y., WANG T., MA L. (2022). Single-Cell Transcriptome Integration Analysis Reveals the Correlation Between Mesenchymal Stromal Cells and Fibroblasts. *Frontiers in Genetics* 13: 798331. <https://doi.org/10.3389/fgene.2022.798331>
- FENG J., MANTESSO A., DE BARI C., NISHIYAMA A., SHARPE P. T. (2011). Dual origin of mesenchymal stem cells contributing to organ growth and repair. *Proceedings of the National Academy of Sciences* 108: 6503-6508. <https://doi.org/10.1073/pnas.1015449108>
- FENG Q., WANG H., NG H. H., ERDJUMENT-BROMAGE H., TEMPST P., STRUHL K., ZHANG Y. (2002). Methylation of H3-Lysine 79 Is Mediated by a New Family of HMTases without a SET Domain. *Current Biology* 12: 1052-1058. [https://doi.org/10.1016/S0960-9822\(02\)00901-6](https://doi.org/10.1016/S0960-9822(02)00901-6)
- FENG Y., YANG Y., ORTEGA M. M., COPELAND J. N., ZHANG M., JACOB J. B., FIELDS T. A., VIVIAN J. L., FIELDS P. E. (2010). Early mammalian erythropoiesis requires the Dot1L methyltransferase. *Blood* 116: 4483-4491. <https://doi.org/10.1182/blood-2010-03-276501>
- FERRARI F., ARRIGONI L., FRANZ H., IZZO A., BUTENKO L., TROMPOUKI E., VOGEL T., MANKE T. (2020). DOT1L-mediated murine neuronal differentiation associates with H3K79me2 accumulation and preserves SOX2-enhancer accessibility. *Nature Communications* 11: 5200. <https://doi.org/10.1038/s41467-020-19001-7>
- FITZGERALD J., MOUREAU S., DROGARIS P., O'CONNELL E., ABSHIRU N., VERREAU A., THIBAUT P., GRENON M., LOWNDES N. F. (2011). Regulation of the DNA Damage Response and Gene Expression by the Dot1L Histone Methyltransferase and the 53Bp1 Tumour Suppressor. *PLoS ONE* 6: e14714. <https://doi.org/10.1371/journal.pone.0014714>
- FRANZ H., VILLARREAL A., HEIDRICH S., VIDEM P., KILPERT F., MESTRES I., CALEGARI F., BACKOFEN R., MANKE T., VOGEL T. (2019). DOT1L promotes progenitor proliferation and primes neuronal layer identity in the developing cerebral cortex. *Nucleic Acids Research* 47: 168-183. <https://doi.org/10.1093/nar/gky953>
- GODFREY L., CRUMP N. T., O'BYRNES., LAU J. J., RICES., HARMAN J. R., JACKSON T., ELLIOTT N., BUCK G., CONNOR C., THORNER., KNAPP D. J. H. F., HEIDENREICH O., VYAS P., MENENDEZ P., INGLOTT S., ANCLIFF P., GENG H., ROBERTS I., ROY A., MILNE T. A. (2021). H3K79me2/3 controls enhancer-promoter interactions and activation of the pan-cancer stem cell marker PROM1/CD133 in MLL-AF4 leukemia cells. *Leukemia* 35: 90-106. <https://doi.org/10.1038/s41375-020-0808-y>
- GRAY DE CRISTOFORIS A., FERRARI F., CLOTMAN F., VOGEL T. (2020). Differentiation and localization of interneurons in the developing spinal cord depends on DOT1L expression. *Molecular Brain* 13: 85. <https://doi.org/10.1186/s13041-020-00623-3>
- HEMATTI P. (2012). Mesenchymal stromal cells and fibroblasts: a case of mistaken identity?. *Cytotherapy* 14: 516-521. <https://doi.org/10.3109/14653249.2012.677822>
- HERMANS F., HEMERYCK L., LAMBRIGHTS I., BRONCKAERS A., VANKELECOM H. (2021). Intertwined Signaling Pathways Governing Tooth Development: A Give-and-Take Between Canonical Wnt and Shh. *Frontiers in Cell and Developmental Biology* 9: 758203. <https://doi.org/10.3389/fcell.2021.758203>
- IWASAKI K., KOMAKI M., YOKOYAMA N., TANAKA Y., TAKI A., KIMURA Y., TAKEDA M., ODA S., IZUMI Y., MORITA I. (2013). Periodontal Ligament Stem Cells Possess the Characteristics of Pericytes. *Journal of Periodontology* 84: 1425-1433. <https://doi.org/10.1902/jop.2012.120547>
- JONES B., SU H., BHAT A., LEI H., BAJKO J., HEVI S., BALTUS G. A., KADAM S., ZHAI H., VALDEZ R., GONZALO S., ZHANG Y., LI E., CHEN T. (2008). The Histone H3K79 Methyltransferase Dot1L Is Essential for Mammalian Development and Heterochromatin Structure. *PLoS Genetics* 4: e1000190. <https://doi.org/10.1371/journal.pgen.1000190>
- JOSHI P., VIJAYKUMAR A., ENKHMANDAKH B., SHIN D.G., MINA M., BAYARSAIHAN D. (2022a). The chromatin accessibility landscape in the dental pulp of mouse molars and incisors. *Acta Biochimica Polonica* 69: 131-138. [https://doi.org/10.18388/abp.2020\\_5771](https://doi.org/10.18388/abp.2020_5771)
- JOSHI P., VIJAYKUMAR A., ENKHMANDAKH B., MINA M., SHIN D.G., BAYARSAIHAN D. (2022b). Genome-wide distribution of 5hmC in the dental pulp of mouse molars and incisors. *The Journal of Biochemistry* 171: 123-129. <https://doi.org/10.1093/jb/mvab114>
- KAUKUA N., SHAHIDI M. K., KONSTANTINIDOU C., DYACHUK V., KAUCKA M., FURLAN A., AN Z., WANG L., HULTMAN I., ÄHRLUND-RIECHTER L., BLOM H., BRISMAR H., LOPES N. A., PACHNIS V., SUTER U., CLEVERS H., THESLEFF I., SHARPE P., ERNFORS P., FRIED K., ADAMEYKO I. (2014). Glial origin of mesenchymal stem cells in a tooth model system. *Nature* 513: 551-554. <https://doi.org/10.1038/nature13536>
- KIM W., CHOI M., KIM J.E. (2014). The histone methyltransferase Dot1/DOT1L as a critical regulator of the cell cycle. *Cell Cycle* 13: 726-738. <https://doi.org/10.4161/cc.28104>
- KIM S.K., JUNG I., LEE H., KANG K., KIM M., JEONG K., KWON C. S., HAN Y.M., KIM Y. S., KIM D., LEE D. (2012). Human Histone H3K79 Methyltransferase DOT1L Methyltransferase Binds Actively Transcribing RNA Polymerase II to Regulate Gene Expression. *Journal of Biological Chemistry* 287: 39698-39709. <https://doi.org/10.1074/jbc.M112.384057>
- LIAO Y., SMYTH G. K., SHI W. (2014). featureCounts: an efficient general purpose program for assigning sequence reads to genomic features. *Bioinformatics* 30: 923-930. <https://doi.org/10.1093/bioinformatics/btt656>
- LOVE M. I., HUBER W., ANDERS S. (2014). Moderated estimation of fold change and dispersion for RNA-seq data with DESeq2. *Genome Biology* 15: 550. <https://doi.org/10.1186/s13059-014-0550-8>
- MAHMOUDI T., BOJ S. F., HATZIS P., LI V. S. W., TAOUATAS N., VRIES R. G. J., TEUNISSEN H., BEGTHEL H., KORVING J., MOHAMMED S., HECKA J. R., CLEVERERS H. (2010). The Leukemia-Associated Mll10/Af10-Dot1L Are Tcf4/ $\beta$ -Catenin Coactivators Essential for Intestinal Homeostasis. *PLoS Biology* 8: e1000539. <https://doi.org/10.1371/journal.pbio.1000539>
- MALCOM C. A., RATRI A., PIASECKA-SRADER J., BOROSHA S., CHAKRAVARTHI V. P., ALVAREZ N. S., VIVIAN J. L., FIELDS T. A., KARIM RUMI M.A., FIELDS P. E. (2022). Primitive Erythropoiesis in the Mouse is Independent of DOT1L Methyltransferase Activity. *Frontiers in Cell and Developmental Biology* 9: 813503. <https://doi.org/10.3389/fcell.2021.813503>
- MIYAMOTO R., OKUDA H., KANAI A., TAKAHASHI S., KAWAMURA T., MATSUI H., KITAMURA T., KITABAYASHI I., INABA T., YOKOYAMA A. (2020). Activation of CpG-Rich Promoters Mediated by MLL Drives MOZ-Rearranged Leukemia. *Cell Reports* 32: 108200. <https://doi.org/10.1016/j.celrep.2020.108200>
- MOLLENTZE J., DURANDT C., PEPPER M. S. (2021). An In Vitro and In Vivo Comparison of Osteogenic Differentiation of Human Mesenchymal Stromal/Stem Cells. *Stem Cells International* 2021: 1-23. <https://doi.org/10.1155/2021/9919361>
- MONTEAGUDO S., CORNELIS F. M. F., AZNAR-LOPEZ C., YIBMANTASIRI P., GUNS L.A., CARMELIET P., CAILOTTO F., LORIES R. J. (2017). DOT1L safeguards cartilage homeostasis and protects against osteoarthritis. *Nature Communications* 8: 15889. <https://doi.org/10.1038/ncomms15889>

- NGUYEN A. T., ZHANG Y. (2011). The diverse functions of Dot1 and H3K79 methylation. *Genes & Development* 25: 1345-1358. <https://doi.org/10.1101/gad.2057811>
- PANCHO A., AERTS T., MITSOGIANNIS M. D., SEUNTJENSE. (2020). Protocadherins at the Crossroad of Signaling Pathways. *Frontiers in Molecular Neuroscience* 13: 117. <https://doi.org/10.3389/fnmol.2020.00117>
- POLAŃSKI K., YOUNG M. D., MIAO Z., MEYER K. B., TEICHMANN S. A., PARK J.E. (2020). BBKNN: fast batch alignment of single cell transcriptomes. *Bioinformatics* 36: 964-965. <https://doi.org/10.1093/bioinformatics/btz625>
- KRIVANEK J., SOLDATOV R. A., KASTRITI M. E., CHONTOROTZEA T., HERDINA A. N., PETERSEN J., SZAROWSKA B., LANDOVA M., MATEJOVA V. K., HOLLA L. I., KUCHLER U., ZDRILIC I. V., VIJAYKUMAR A., BALIC A., MARANGONI P., KLEIN O. D., NEVES V. C. M., YIANNI V., SHARPE P. T., HARKANY T., METSCHER B. D., BAJÉNOFF M., MINA M., FRIED K., KHARCHENKO P. V., ADAMEYKO I. (2020). Dental cell type atlas reveals stem and differentiated cell types in mouse and human teeth. *Nature Communications* 11: 4816. <https://doi.org/10.1038/s41467-020-18512-7>
- QIN W., LEONHARDT H., PICHLER G. (2011). Regulation of DNA methyltransferase 1 by interactions and modifications. *Nucleus* 2: 392-402. <https://doi.org/10.4161/nucl.2.5.17928>
- SANZ-NAVARRO M., SEIDEL K., SUN Z., BERTONNIER-BROUTY L., AMENDT B. A., KLEIN O. D., MICHON F. (2018). Plasticity within the niche ensures the maintenance of a Sox2 + stem cell population in the mouse incisor. *Development* 145: dev155929. <https://doi.org/10.1242/dev.155929>
- SARNO F., NEBBIOSO A., ALTUCCI L. (2020). DOT1L: a key target in normal chromatin remodelling and in mixed-lineage leukaemia treatment. *Epigenetics* 15: 439-453. <https://doi.org/10.1080/15592294.2019.1699991>
- SATIJA R., FARRELL J. A., GENNERT D., SCHIER A. F., REGEV A. (2015). Spatial reconstruction of single-cell gene expression data. *Nature Biotechnology* 33: 495-502. <https://doi.org/10.1038/nbt.3192>
- SHAH S., HENRIKSEN M. A. (2011). A Novel Disrupter of Telomere Silencing 1-like (DOT1L) Interaction Is Required for Signal Transducer and Activator of Transcription 1 (STAT1)-activated Gene Expression. *Journal of Biological Chemistry* 286: 41195-41204. <https://doi.org/10.1074/jbc.M111.284190>
- SIMÕES-COSTA M., BRONNER M. E. (2015). Establishing neural crest identity: a gene regulatory recipe. *Development* 142: 242-257. <https://doi.org/10.1242/dev.105445>
- SOLIMAN H., THERET M., SCOTT W., HILL L., UNDERHILL T. M., HINZ B., ROSSI F. M.V. (2021). Multipotent stromal cells: One name, multiple identities. *Cell Stem Cell* 28: 1690-1707. <https://doi.org/10.1016/j.stem.2021.09.001>
- SOUNDARARAJAN M., KANNAN S. (2018). Fibroblasts and mesenchymal stem cells: Two sides of the same coin?. *Journal of Cellular Physiology* 233: 9099-9109. <https://doi.org/10.1002/jcp.26860>
- SKUCHA A., EBNER J., SCHMÖLLERL J., ROTH M., EDER T., CÉSAR-RAZQUIN A., STUKALOV A., VITTORI S., MUHAR M., LU B., AICHINGER M., JUDE J., MÜLLER A. C., GYÖRFFY B., VAKOC C. R., VALENT P., BENNETT K. L., ZUBER J., SUPERTI-FURGA G., GREBIEN F. (2018). MLL-fusion-driven leukemia requires SETD2 to safeguard genomic integrity. *Nature Communications* 9: 1983. <https://doi.org/10.1038/s41467-018-04329-y>
- STEGER D. J., LEFTEROVA M. I., YING L., STONESTROM A. J., SCHUPP M., ZHUO D., VAKOC A. L., KIM J.E., CHEN J., LAZAR M. A., BLOBEL G. A., VAKOC C. R. (2008). DOT1L/KMT4 Recruitment and H3K79 Methylation Are Ubiquitously Coupled with Gene Transcription in Mammalian Cells. *Molecular and Cellular Biology* 28: 2825-2839. <https://doi.org/10.1128/MCB.02076-07>
- SUI B., CHEN C., KOU X., LI B., XUAN K., SHI S., JIN Y. (2019). Pulp Stem Cell-Mediated Functional Pulp Regeneration. *Journal of Dental Research* 98: 27-35. <https://doi.org/10.1177/0022034518808754>
- SUTTER P. A., KARKIS, CRAWLEY I., SINGH V., BERNT K. M., ROWE D. W., CROCKER S. J., BAYARSAIHAND, GUZZO R. M. (2021). Mesenchyme-specific loss of Dot1L histone methyltransferase leads to skeletal dysplasia phenotype in mice. *Bone* 142: 115677. <https://doi.org/10.1016/j.bone.2020.115677>
- TRAAG V. A., WALTMAN L., VAN ECK N. J. (2019). From Louvain to Leiden: guaranteeing well-connected communities. *Scientific Reports* 9: 5233. <https://doi.org/10.1038/s41598-019-41695-z>
- TSUTSUI T. (2020). Dental Pulp Stem Cells: Advances to Applications. *Stem Cells and Cloning: Advances and Applications* Volume 13: 33-42. <https://doi.org/10.2147/SCCAA.S166759>
- VAN WIJNEN A. J., BAGHERI L., BADRELDIN A. A., LARSON A. N., DUDAKOVIC A., THALER R., PARADISE C. R., WU Z. (2021). Biological functions of chromobox (CBX) proteins in stem cell self-renewal, lineage-commitment, cancer and development. *Bone* 143: 115659. <https://doi.org/10.1016/j.bone.2020.115659>
- VLAMING H., VAN LEEUWEN F. (2016). The upstreams and downstreams of H3K79 methylation by DOT1L. *Chromosoma* 125: 593-605. <https://doi.org/10.1007/s00412-015-0570-5>
- WAKEMAN T. P., WANG Q., FENG J., WANG X.F. (2012). Bat3 facilitates H3K79 dimethylation by DOT1L and promotes DNA damage-induced 53BP1 foci at G1/G2 cell-cycle phases. *The EMBO Journal* 31: 2169-2181. <https://doi.org/10.1038/emboj.2012.50>
- WEIRICH S., KHELLA M. S., JELTSCH A. (2021). Structure, Activity and Function of the Suv39h1 and Suv39h2 Protein Lysine Methyltransferases. *Life* 11: 703. <https://doi.org/10.3390/life11070703>
- WOLF F. A., ANGERER P., THEIS F. J. (2018). SCANPY: large-scale single-cell gene expression data analysis. *Genome Biology* 19: 15. <https://doi.org/10.1186/s13059-017-1382-0>
- WU A., ZHI J., TIAN T., CIHAN A., CEVHER M. A., LIU Z., DAVID Y., MUIR T. W., ROEDER R. G., YU M. (2021). DOT1L complex regulates transcriptional initiation in human erythroleukemic cells. *Proceedings of the National Academy of Sciences* 118: e2106148118. <https://doi.org/10.1073/pnas.2106148118>
- YANG L., LEI Q., LI L., YANG J., DONG Z., CUI H. (2019). Silencing or inhibition of H3K79 methyltransferase DOT1L induces cell cycle arrest by epigenetically modulating c-Myc expression in colorectal cancer. *Clinical Epigenetics* 11: 199. <https://doi.org/10.1186/s13148-019-0778-y>
- YOO H., LEE Y. J., PARK C., SON D., CHOI D. Y., PARK J.H., CHOI H.J., LA H. W., CHOI Y.J., MOON E.H., SAUR D., CHUNG H. M., SONG H., DO J. T., JANG H., LEE D. R., PARK C., LEE O.H., CHO S.G., HONG S.H., KONG G., KIM J.H., CHOI Y., HONG K. (2020). Epigenetic priming by Dot1l in lymphatic endothelial progenitors ensures normal lymphatic development and function. *Cell Death & Disease* 11: 14. <https://doi.org/10.1038/s41419-019-2201-1>
- ZHANG Y. D., CHEN Z., SONG Y. Q., LIU C., CHEN Y. P. (2005). Making a tooth: growth factors, transcription factors, and stem cells. *Cell Research* 15: 301-316. <https://doi.org/10.1038/sj.cr.7290299>
- ZHANG Y., LIU T., MEYER C. A., ECKHOUTE J., JOHNSON D. S., BERNSTEIN B. E., NUSBAUM C., MYERS R. M., BROWN M., LI W., LIU X. S. (2008). Model-based Analysis of ChIP-Seq (MACS). *Genome Biology* 9: R137. <https://doi.org/10.1186/gb-2008-9-9-r137>
- ZHAO H., FENG J., SEIDEL K., SHI S., KLEIN O., SHARPE P., CHAI Y. (2014). Secretion of Shh by a Neurovascular Bundle Niche Supports Mesenchymal Stem Cell Homeostasis in the Adult Mouse Incisor. *Cell Stem Cell* 14: 160-173. <https://doi.org/10.1016/j.stem.2013.12.013>
- ZHAO L., ZHANG P., GALBO P. M., ZHOU X., ARYAL S., QIU S., ZHANG H., ZHOU Y., LI C., ZHENG D., BHATIA R., LU R. (2021). Transcription factor MEF2D is required for the maintenance of MLL-rearranged acute myeloid leukemia. *Blood Advances* 5: 4727-4740. <https://doi.org/10.1182/bloodadvances.2021004469>
- ZHENG G. X. Y., TERRY J. M., BELGRADER P., RYVKIN P., BENT Z. W., WILSON R., ZIRALDO S. B., WHEELER T. D., MCDERMOTT G. P., ZHU J., GREGORY M. T., SHUGA J., MONTESCLAROS L., UNDERWOOD J. G., MASQUELIER D. A., NISHIMURA S. Y., SCHNALL-LEVIN M., WYATT P. W., HINDSON C. M., BHARADWAJ R., WONG A., NESS K. D., BEPPU L. W., DEEG H. J., MCFARLAND C., LOEB K. R., VALENTE W. J., ERICSON N. G., STEVENS E. A., RADICH J. P., MIKKELSEN T. S., HINDSON B. J., BIELAS J. H. (2017). Massively parallel digital transcriptional profiling of single cells. *Nature Communications* 8: 14049. <https://doi.org/10.1038/ncomms14049>